

Nucleation Mechanisms of Molecular Oxides: A Study of the Assembly–Disassembly of $[W_6O_{19}]^{2-}$ by Theory and Mass Spectrometry**

Laia Vilà-Nadal, Antonio Rodríguez-Forteza,* Li-Kai Yan, Elizabeth F. Wilson, Leroy Cronin,* and Josep M. Poble†

Polyoxometalates (POMs) are a vast class of polynuclear molecular oxide anions usually formed by W, Mo, or V.^[1] These clusters are interesting since their assembly through polymerized metal-based polyhedra can yield molecules that span the molecular to nanoparticle size range^[2a] and form colloidal aggregates.^[2b] This capacity to span large size ranges, coupled with their attractive electronic and molecular properties,^[1] gives rise to a variety of applications in diverse fields such as catalysis, medicine, and materials science.^[3]

Despite the ever-increasing interest in this class of materials,^[1–3] accurate determination of the formula, structure, and building-block principles still represents a great challenge for understanding and exploiting cluster formation. To this end the use of electrospray mass spectrometry (ESIMS) to investigate POM systems, as a complementary technique to X-ray crystallography and NMR studies, has increased steadily over the last decade.^[4] Recently, Cronin and co-workers demonstrated that electrospray (ESI) and cryospray mass spectrometry (CSIMS) can be used as versatile tools in various complex systems to investigate the molecular oxide clusters in solution, allowing elucidation of the formula and providing insight into the “building-block” species present in solution.^[5]

Considerable theoretical research concerning POMs has been carried out during the last decade,^[6] but only a few

studies have been devoted to analysis of their mechanism of formation. Kepert, in the early 1960s, suggested that formation of POMs might involve the addition of WO_4 tetrahedra. The first step would imply the addition of a WO_4 unit, acting as a bidentate ligand, to a second WO_4 unit by expanding the coordination number of the latter metal ion to six.^[7,8] Acidification of alkaline aqueous solutions of simple oxo anions is one of the most common preparative methods of POMs.^[7] After protonation, the W^{VI} ion becomes more electrophilic and can be more effectively attacked by the nucleophilic O atoms of the $[WO_4]^{2-}$ anion. In the 1970s, Tytko and Glemser proposed elaborate mechanisms to explain the formation of POMs based on the Kepert addition process.^[9] There is, however, little experimental evidence to support these mechanisms.^[7] To the best of our knowledge, no other theoretical studies have attempted to elucidate the formation mechanisms of POMs. Only studies about the rates of oxygen exchange between the Lindqvist anion $[H_xM_6O_{19}]^{(8-x)-}$ ($M = Nb, Ta$) and aqueous solutions which show the reversibility of the M–O bond breaking and formation are available.^[10] Herein, we aim to shed light on the formation mechanisms of POMs with low nuclearities, as is the case of the W-based Lindqvist anion $[W_6O_{19}]^{2-}$, under different pH conditions. To achieve this goal, we performed ESIMS experiments on $[(C_4H_9)_4N]_2W_6O_{19}^{[11]}$ combined with computational techniques that include the effect of the solvent in two different ways, either through a continuum model in standard DFT methods or as explicit molecules by means of Car–Parrinello molecular-dynamics (MD) simulations. Since the ESIMS experiments can provide fragmentation data, the correlation between these data and the mechanistic details could provide important information if the species observed in the fragmentation process can be related to those generated in the formation of the POM cluster.

To analyze the first step of the growth mechanism, we performed Car–Parrinello MD simulations. The metadynamics approach was used to accelerate the dynamics and to compute the free-energy barriers.^[12] Such a computational strategy has been already applied to the study of the hydration of hydrogentungstate anions under different pH conditions.^[13] The hydrogentungstate anion $[WO_3(OH)]^-$ is considered as the building block in our construction scheme as it is an abundant species under the conditions in which POMs are synthesized.^[7] We present a qualitative description of the events observed during an 11 ps metadynamics run of

[*] L. Vilà-Nadal, Dr. A. Rodríguez-Forteza, Dr. L.-K. Yan,^[†] Prof. Dr. J. M. Poble
Departament de Química Física i Inorgànica, Universitat Rovira i Virgili, c/Marcel·lí Domingo s/n, 43007 Tarragona (Spain)
Fax: (+34) 977-559-569
E-mail: antonio.rodriguez@urv.cat
josepmaria.poble@urv.cat

E. F. Wilson, Prof. Dr. L. Cronin
Department of Chemistry, The University of Glasgow
University Avenue, Glasgow G12 8QQ, Scotland (UK)
Fax: (+44) 141-330-4888
E-mail: l.cronin@chem.gla.ac.uk

[†] Current Address: Institute of Functional Material Chemistry
Department of Chemistry, Northeast Normal University
Changchun 130024 (China).

[**] We acknowledge support from the MEC of Spain (project CTQ2008-06549-C02-01/BQU and the Ramón y Cajal Program (A.R.F.)), the DGR of the Autonomous Government of Catalonia (2005SGR-00104), the EPSRC, and Bruker Daltonics. Part of the computer resources were provided by the Barcelona Supercomputing Center (Centro Nacional de Supercomputación).

Supporting information for this article is available on the WWW under <http://dx.doi.org/10.1002/anie.200901348>.

the system formed by 2 $[\text{WO}_3(\text{OH})]^-$ monomers and 27 H_2O molecules.^[14]

Firstly, we observe H^+ transfer from one $[\text{WO}_3(\text{OH})]^-$ monomer to the other, indicating that H^+ transfer processes between monomers, when they are close enough, are highly probable. At about 0.6 ps, dimerization takes place to yield a structure in which one W atom is four-coordinated and the other W is five-coordinated (a **5c-4c** structure, see Figure 1).

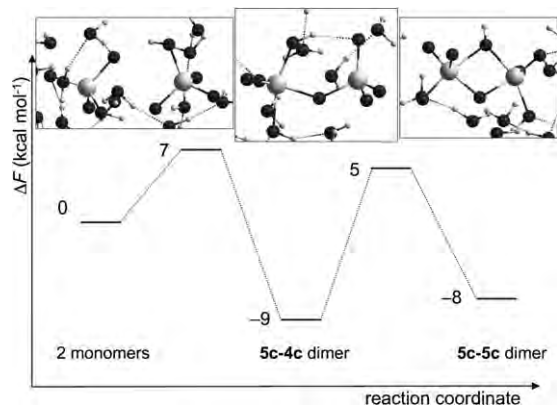


Figure 1. Free-energy profile corresponding to the formation of dinuclear $[\text{W}_2\text{O}_6(\text{OH})_2]^{2-}$ species.

Afterwards, we observed the formation of a **5c-5c** structure that remains for around 3.5 ps. Finally, we observed recrossings to the **5c-4c** structure and to the two monomers. The free-energy surface (FES) explored by the metadynamics run can be evaluated directly through the added time-dependent potential. Such a method has been proved to be a reasonable approximation to the free-energy barrier, ΔF^\ddagger .^[15] The free-energy profile is depicted in Figure 1.

The process with the lowest barrier is the formation of the **5c-4c** structure from the two $[\text{WO}_3(\text{OH})]^-$ monomers ($7 \pm 3 \text{ kcal mol}^{-1}$). From the **5c-4c** minimum well, the system can escape to the **5c-5c** well or come back to form the monomers; both processes show similar probability (within the uncertainty). All these barriers can be easily overcome at the temperatures at which POMs are formed (ambient temperature or even higher). The **5c-4c** structure is around $9 \pm 3 \text{ kcal mol}^{-1}$ more stable than the system formed by the two monomers and the water molecules. Structure **5c-5c** is almost degenerate with structure **5c-4c**. An interesting point is that during the metadynamics, we did not observe the **6c-4c** structure proposed by Kepert. Thus, this type of dimer, if it exists, must show a higher barrier than the **5c-4c** and **5c-5c** structures. Geometry optimization at the standard DFT/COSMO level confirms that the Kepert structure is not stable. Additional metadynamics (MTD) runs using other sets of collective variables (CV) were also performed, and the main features of the previous simulation were retrieved (see the Supporting Information).

Since tungstate anions can also be present in the solution, a metadynamics run including $[\text{WO}_3(\text{OH})]^-$, $[\text{WO}_4]^{2-}$, and 27 H_2O molecules was also performed (see the Supporting Information). The O atoms of the tungstate anion are more

nucleophilic than those of the hydrogentungstate. Therefore, the barrier to form the $[\text{W}_2\text{O}_7(\text{OH})]^{3-}$ dimer should be smaller than for $[\text{W}_2\text{O}_6(\text{OH})_2]^{2-}$. Indeed, dimerization to a **5c-4c** structure is observed in a standard Car-Parrinello simulation without accelerating the dynamics, that is, a low energy barrier must exist. The free-energy barrier estimated from a metadynamics run is only 4 kcal mol^{-1} , and the stability of dimer $[\text{W}_2\text{O}_7(\text{OH})]^{3-}$ with respect to the monomers is 9 kcal mol^{-1} . Once formed, this species will most likely be protonated, owing to the high density charge present at the O atoms, thus yielding the same type of dimer as if two hydrogentungstate anions were dimerized.

The effect of pH value on the formation of dinuclear species was also analyzed by simulations under low pH conditions with 2 $\text{WO}_2(\text{OH})_2$ monomers surrounded by 27 H_2O molecules. In a standard Car-Parrinello MD simulation, we have observed the formation of a hydrated **5c-4c** structure. Thus, we can infer that the dimerization process is highly probable at these conditions. In a 16 ps metadynamics run (see the Supporting Information), we observed intramolecular H^+ transfer to form an aqua ligand, which is released as a water molecule to the bulk solution to yield the dimer $[\text{W}_2\text{O}_6(\text{OH})]^-$. The estimated free-energy barrier for this process is $8 \pm 2 \text{ kcal mol}^{-1}$ (compared with $23 \pm 1 \text{ kcal mol}^{-1}$ under medium pH conditions, see the Supporting Information). The **5c-5c** structure is also formed from the **5c-4c** dimer; the free-energy barrier is somewhat smaller than that at mildly acidic conditions ($11 \pm 2 \text{ kcal mol}^{-1}$). In this simulation also, the Kepert structure was not observed. Moreover, we observed that hydration, that is, coordination of water molecules to the W^{VI} ions, gives extra stability to dimers. This result is in good agreement with the fact that the larger the number of protons attached to the dimer, that is, the electrophilicity of W^{VI} ions, the larger the tendency to be attacked by nucleophilic water molecules.^[13] Therefore, it can be concluded that under low pH conditions formation of dinuclear species is favored. Moreover, clusters with higher levels of hydration are preferred to water-free structures.

On the basis of the consecutive steps of nucleation and water condensation, two mechanisms for the formation of the Lindqvist anion consistent with the ESIMS fragmentation experiments may be put forward (M1 and M2, Tables 1 and 2, respectively). The peaks observed in the ESIMS experiments (Table S2 in the Supporting Information and Figure 2) are

Table 1: Proposed mechanism (M1) for the formation of the Lindqvist anion $[\text{W}_6\text{O}_{19}]^{2-}$.^[a] The species detected in ESIMS experiments are highlighted in bold.

1) $[\text{WO}_3(\text{OH})]^-_{(\text{aq})} + [\text{WO}_3(\text{OH})]^-_{(\text{aq})} \rightarrow [\text{W}_2\text{O}_6(\text{OH})_2]^{2-}_{(\text{aq})}$	-7.4
2) $[\text{W}_2\text{O}_6(\text{OH})_2]^{2-}_{(\text{aq})} \rightarrow [\text{W}_2\text{O}_7]^{2-}_{(\text{aq})} + \text{H}_2\text{O}_{(\text{aq})}$	+3.0
3) $[\text{W}_2\text{O}_7]^{2-}_{(\text{aq})} + [\text{WO}_3(\text{OH})]^-_{(\text{aq})} \rightarrow [\text{W}_3\text{O}_{10}(\text{OH})]^{3-}_{(\text{aq})}$	-3.7
4) $[\text{W}_3\text{O}_{10}(\text{OH})]^{3-}_{(\text{aq})} + \text{H}_3\text{O}^+_{(\text{aq})} \rightarrow [\text{W}_3\text{O}_{10}]^{2-}_{(\text{aq})} + 2 \text{H}_2\text{O}_{(\text{aq})}$	+2.0
5) $[\text{W}_3\text{O}_{10}]^{2-}_{(\text{aq})} + [\text{WO}_3(\text{OH})]^-_{(\text{aq})} \rightarrow [\text{W}_4\text{O}_{13}(\text{OH})]^{3-}_{(\text{aq})}$	-18.5
6) $[\text{W}_4\text{O}_{13}(\text{OH})]^{3-}_{(\text{aq})} + \text{H}_3\text{O}^+_{(\text{aq})} \rightarrow [\text{W}_4\text{O}_{13}]^{2-}_{(\text{aq})} + 2 \text{H}_2\text{O}_{(\text{aq})}$	-14.9
7) $[\text{W}_4\text{O}_{13}]^{2-}_{(\text{aq})} + [\text{WO}_3(\text{OH})]^-_{(\text{aq})} \rightarrow [\text{W}_5\text{O}_{16}(\text{OH})]^{3-}_{(\text{aq})}$	-2.5
8) $[\text{W}_5\text{O}_{16}(\text{OH})]^{3-}_{(\text{aq})} + \text{H}_3\text{O}^+_{(\text{aq})} \rightarrow [\text{W}_5\text{O}_{16}]^{2-}_{(\text{aq})} + 2 \text{H}_2\text{O}_{(\text{aq})}$	+3.8
9) $[\text{W}_5\text{O}_{16}]^{2-}_{(\text{aq})} + [\text{WO}_3(\text{OH})]^-_{(\text{aq})} \rightarrow [\text{W}_6\text{O}_{19}(\text{OH})]^{3-}_{(\text{aq})}$	-24.2
10) $[\text{W}_6\text{O}_{19}(\text{OH})]^{3-}_{(\text{aq})} + \text{H}_3\text{O}^+_{(\text{aq})} \rightarrow [\text{W}_6\text{O}_{19}]^{2-}_{(\text{aq})} + 2 \text{H}_2\text{O}_{(\text{aq})}$	-34.7

[a] Reaction energies are in kcal mol^{-1} .

Table 2: Proposed mechanism (M2) for the formation of the Lindqvist anion $[\text{W}_6\text{O}_{19}]^{2-}$.^[a] The species detected in ESIMS experiments are highlighted in bold.

1) $[\text{WO}_3(\text{OH})]^-_{(\text{aq})} + [\text{WO}_3(\text{OH})]^-_{(\text{aq})} \rightarrow [\text{W}_2\text{O}_6(\text{OH})_2]^{2-}_{(\text{aq})}$	-7.4
2) $[\text{W}_2\text{O}_6(\text{OH})_2]^{2-}_{(\text{aq})} + \text{H}_3\text{O}^+_{(\text{aq})} \rightarrow [\text{W}_2\text{O}_6(\text{OH})]^-_{(\text{aq})} + 2\text{H}_2\text{O}_{(\text{aq})}$	-14.4
3) $[\text{W}_2\text{O}_6(\text{OH})]^-_{(\text{aq})} + [\text{WO}_3(\text{OH})]^-_{(\text{aq})} \rightarrow [\text{W}_3\text{O}_9(\text{OH})_2]^{2-}_{(\text{aq})}$	-8.7
4) $[\text{W}_3\text{O}_9(\text{OH})_2]^{2-}_{(\text{aq})} + \text{H}_3\text{O}^+_{(\text{aq})} \rightarrow [\text{W}_3\text{O}_9(\text{OH})]^-_{(\text{aq})} + 2\text{H}_2\text{O}_{(\text{aq})}$	+3.0
5) $[\text{W}_3\text{O}_9(\text{OH})]^-_{(\text{aq})} + [\text{WO}_3(\text{OH})]^-_{(\text{aq})} \rightarrow [\text{W}_4\text{O}_{12}(\text{OH})_2]^{2-}_{(\text{aq})}$	-18.8
6) $[\text{W}_4\text{O}_{12}(\text{OH})_2]^{2-}_{(\text{aq})} + \text{H}_3\text{O}^+_{(\text{aq})} \rightarrow [\text{W}_4\text{O}_{12}(\text{OH})]^-_{(\text{aq})} + 2\text{H}_2\text{O}_{(\text{aq})}$	-17.2
7) $[\text{W}_4\text{O}_{12}(\text{OH})]^-_{(\text{aq})} + [\text{WO}_3(\text{OH})]^-_{(\text{aq})} \rightarrow [\text{W}_5\text{O}_{15}(\text{OH})_2]^{2-}_{(\text{aq})}$	+11.4
8) $[\text{W}_5\text{O}_{15}(\text{OH})_2]^{2-}_{(\text{aq})} + \text{H}_3\text{O}^+_{(\text{aq})} \rightarrow [\text{W}_5\text{O}_{15}(\text{OH})]^-_{(\text{aq})} + 2\text{H}_2\text{O}_{(\text{aq})}$	+2.8
9) $[\text{W}_5\text{O}_{15}(\text{OH})]^-_{(\text{aq})} + [\text{WO}_3(\text{OH})]^-_{(\text{aq})} \rightarrow [\text{W}_6\text{O}_{18}(\text{OH})_2]^{2-}_{(\text{aq})}$	-31.9
10) $[\text{W}_6\text{O}_{18}(\text{OH})_2]^{2-}_{(\text{aq})} \rightarrow [\text{W}_6\text{O}_{19}]^{2-}_{(\text{aq})} + \text{H}_2\text{O}_{(\text{aq})}$	-15.7

[a] Reaction energies are in kcal mol^{-1} .

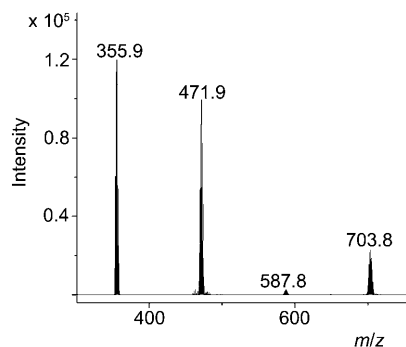


Figure 2. Mass spectral data from MS run B recorded by collision-induced dissociation (CID) of the isolated $[\text{W}_6\text{O}_{19}]^{2-}$ peak at m/z 703.8 (see the Supporting Information for more details). The fragment peaks shown are associated with the species $[\text{W}_3\text{O}_{10}]^{2-}$ (m/z 355.9), $[\text{W}_4\text{O}_{13}]^{2-}$ (m/z 471.9), and $[\text{W}_5\text{O}_{16}]^{2-}$ (m/z 587.8).

associated with the species $[\text{WO}_3(\text{OH})]^-$, $[\text{W}_2\text{O}_7]^{2-}$, $[\text{W}_2\text{O}_6(\text{OH})]^-$, $[\text{W}_3\text{O}_{10}]^{2-}$, $[\text{W}_3\text{O}_9(\text{OH})]^-$, $[\text{W}_4\text{O}_{13}]^{2-}$, $[\text{W}_4\text{O}_{12}(\text{OH})]^-$, $[\text{W}_5\text{O}_{16}]^{2-}$, $[\text{W}_6\text{O}_{19}]^{2-}$, and $[\text{W}_6\text{O}_{18}(\text{OH})]^-$. For each of the stoichiometries, the lowest-energy structure was sought (see the Supporting Information). The dinuclear species with $[\text{W}_2\text{O}_6(\text{OH})_2]^{2-}$ stoichiometry, which are predicted to be formed in the first step of aggregation, should undergo dehydration to $[\text{W}_2\text{O}_7]^{2-}$ (M1, step 2) or, after protonation, to $[\text{W}_2\text{O}_6(\text{OH})]^-$ (M2, step 2) to be consistent with the ESIMS results. Under low pH conditions, dehydration is predicted to have a free-energy barrier of only 8 kcal mol^{-1} (see above), which is consistent with experimental observations.

Potential structures for tri-, tetra-, penta-, and hexanuclear species with the same stoichiometries as those observed in the ESIMS experiments are depicted in Figure 3. The structures corresponding to stoichiometries derived from mechanism M2 are almost identical to those shown in Figure 3 with an extra H atom.

For $[\text{W}_3\text{O}_{10}]^{2-}$, a symmetric and compact structure with a tricoordinate O atom ($\mu_3\text{-O}$) is found. Interestingly, this peculiar structure is the same as that found recently by Müller and co-workers for a trinuclear $[\text{W}_3\text{O}_{10}]^{2-}$ cluster in the cavity of a Mo/W-storage protein.^[16] At our computational level, the formation of these species (M1 and M2) is slightly endothermic. For $[\text{W}_4\text{O}_{13}]^{2-}$, a compact structure with a $\mu_3\text{-O}$ atom,

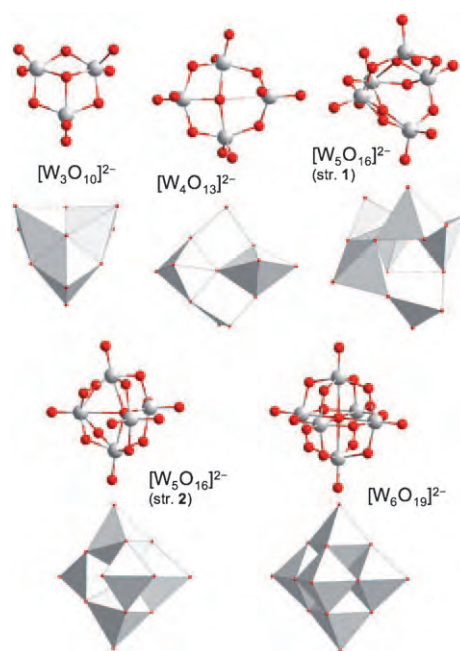


Figure 3. Polyhedral and ball-and-stick representations of the most stable structures found at the BP86/COSMO level for the stoichiometries observed in the ESIMS experiments.

which could also be considered as $\mu_4\text{-O}$ because the distance between the central O atom and the fourth W atom is less than 3 \AA , was found to have the lowest energy among the structures that we examined. This structure already contains one of the three W_4O_4 rings of the Lindqvist anion. The formation of tetranuclear clusters is moderately exothermic, which is in good agreement with the fact that only tetranuclear species were observed along with the Lindqvist anion when the ESIMS experiment (run D) was carried out without selected-ion collision-induced dissociation (CID) in the MS collision cell (see Figure 4 and Table S1 in the Supporting Information for MS parameters). In contrast, the formation of pentanuclear structures is predicted to be endothermic, especially through mechanism M2. Indeed, none of the pentanuclear species proposed in M2 were observed in the ESIMS experiments.

For the only pentanuclear cluster observed ($[\text{W}_5\text{O}_{16}]^{2-}$), two structures with similar energy were found (structures 1

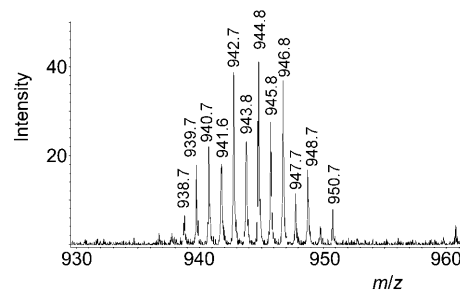


Figure 4. Spectral data from MS run D (see the Supporting Information for more details) showing the peak associated with the species $[\text{W}_4\text{O}_{13}\text{H}]^-$ at m/z 944.8. This species was formed without selected-ion CID fragmentation.

and **2** in Figure 3). Structure **1** features two μ_3 -O atoms, each within a planar W_3 unit as in the tetranuclear cluster. These planar trinuclear motifs, also present in the Lindqvist anion and in the tetranuclear form, confer stability to the cluster. Structure **2**, which is only 3 kcal mol⁻¹ less stable than structure **1** and with a μ_5 -O atom, shows a framework that fairly resembles that of the Lindqvist anion (see Figure 3). Although structure **1** is slightly more stable than structure **2**, the topology of the latter seems more favorable to lead to the hexametalate. The most exothermic steps of those proposed are the formation of the hexanuclear species, especially for mechanism M1.

In summary, the combined use of ESIMS fragmentation experiments and complementary DFT approaches provides deeper insight into the formation mechanisms of POMs with low nuclearities. The dinuclear structure proposed by Kepert was not found to be stable. Other structures in which the W atoms are four- or fivefold coordinated are predicted by DFT methods to be the most stable. Moreover, Car–Parrinello MD simulations show that the coordination sphere of W atoms might be expanded by direct interaction with water molecules. We postulate that once the dinuclear species have been formed, successive steps of protonation and water condensation with subsequent aggregation occur (mechanisms M1 and M2) to justify the clusters detected in the ESIMS experiments. An energetic cascade profile is predicted for both mechanisms with the last steps being the most exothermic. Therefore, it is proposed that the Lindqvist anion is formed by consecutive steps that incorporate one metal unit at a time. For the most-stable tetra- and pentanuclear intermediate clusters, planar W_3 building blocks have been identified which confer this high stability on these intermediate clusters. The complementarity between theory and experiment provides important clues about the formation steps of the Lindqvist anion. This study represents the first real approach to understanding the aggregation mechanisms of a molecular oxide. There is, however, a long way to go. We hope that analogous studies for other iso-polyoxo anions and especially for hetero-polyoxo anions $[XMyO_z]^{q-}$ will provide new insight into the rationalization of these processes, which are fundamental in the formation of nanostructures based on oxometalates.

Experimental Section

For the ESIMS experiments, $[(n-C_4H_9)_4N]_2W_6O_{19}$ was synthesized from $[(n-C_4H_9)_4N]_2W_{10}O_{32}$ by following the method of Klemperer and co-workers,^[11] and its identity was confirmed by single-crystal X-ray diffraction and elemental analysis. Elemental analysis (%) calcd for $C_{32}H_{72}N_2W_6O_{19}$ (1892.0 g mol⁻¹): C 20.31, H 3.84, N 1.48; found: C 20.28, H 3.76, N 1.50. The MS samples were prepared by dissolution of 10 mg $[(n-C_4H_9)_4N]_2W_6O_{19}$ in 5 mL MeCN and sonication for 15 min; 20 μ L of this solution was made up to 4 mL with MeCN. All MS data were collected using a Q-trap, time-of-flight MS (MicrOTOF-Q MS) instrument equipped with an electrospray (ESI) source supplied by Bruker Daltonics Ltd. The detector was a time-of-flight, micro-channel plate detector, and all data were processed by using the Bruker Daltonics Data Analysis 4.0 software; simulated isotope patterns were investigated with Bruker Isotope Pattern software and Molecular Weight Calculator 6.45. See the Supporting Information

for more details on MS parameters and the data collection runs carried out.

Computational methodology: The static calculations were carried out by using DFT methodology with the ADF 2004 program.^[17] The exchange-correlation functionals of Becke and Perdew were used.^[18] Triple- ζ polarization basis sets were employed to describe the valence electrons of W, O, and H. All the structures were fully optimized in the presence of a continuous model solvent by means of the conductor-like screening model (COSMO).^[19] The MD simulations were performed at DFT level by means of the CPMD program package.^[20] The description of the electronic structure is based on the expansion of the valence electronic wave functions into a plane wave basis set (energy cutoff of 70 Ry). The interaction between the valence electrons and the ionic cores was treated through the pseudopotential approximation.^[21] We adopted the generalized gradient-corrected Becke–Lee–Yang–Parr (BLYP) exchange-correlation functional.^[18] See the Supporting Information for more details on the computational settings.

Received: March 10, 2009

Revised: April 24, 2009

Published online: June 18, 2009

Keywords: Lindqvist anion · mass spectrometry · nucleation · polyoxometalates · tungsten

- [1] D.-L. Long, E. Burkholder, L. Cronin, *Chem. Soc. Rev.* **2007**, 36, 105.
- [2] a) A. Müller, E. Beckmann, H. Bögge, M. Schmidtman, A. Dress, *Angew. Chem.* **2002**, 114, 1210; *Angew. Chem. Int. Ed.* **2002**, 41, 1162; b) T. Liu, *J. Am. Chem. Soc.* **2003**, 125, 312.
- [3] a) J. T. Rhule, W. A. Neiwert, K. I. Hardcastle, B. T. Do, C. L. Hill, *J. Am. Chem. Soc.* **2001**, 123, 12101; b) B. Hasenknopf, *Front. Biosci.* **2005**, 10, 275; c) C. J. Jiang, A. Lesbani, R. Kawamoto, S. Uchida, N. Mizuno, *J. Am. Chem. Soc.* **2006**, 128, 14240.
- [4] a) M. J. Deery, O. W. Howarth, K. R. Jennings, *J. Chem. Soc. Dalton Trans.* **1997**, 4783; b) T. Waters, R. A. J. O'Hair, A. G. Wedd, *J. Am. Chem. Soc.* **2003**, 125, 3384; c) C. A. Ohlin, E. M. Villa, J. C. Fettinger, W. H. Casey, *Angew. Chem.* **2008**, 120, 8375; *Angew. Chem. Int. Ed.* **2008**, 47, 8251.
- [5] a) E. F. Wilson, H. Abbas, B. J. Duncombe, C. Streb, D.-L. Long, L. Cronin, *J. Am. Chem. Soc.* **2008**, 130, 13876; b) C. P. Pradeep, D.-L. Long, G. N. Newton, Y.-F. Song, L. Cronin, *Angew. Chem.* **2008**, 120, 4460; *Angew. Chem. Int. Ed.* **2008**, 47, 4388; c) D.-L. Long, C. Streb, Y. F. Song, S. Mitchell, L. Cronin, *J. Am. Chem. Soc.* **2008**, 130, 1830; d) H. N. Miras, J. Yan, D.-L. Long, L. Cronin, *Angew. Chem.* **2008**, 120, 8548; *Angew. Chem. Int. Ed.* **2008**, 47, 8420.
- [6] a) J. M. Poblet, X. Lopez, C. Bo, *Chem. Soc. Rev.* **2003**, 32, 297; b) A. Bagno, M. Bonchio, *Angew. Chem.* **2005**, 117, 2059; *Angew. Chem. Int. Ed.* **2005**, 44, 2023; c) L.-K. Yan, X. López, J. J. Carbó, R. Sniatynsky, D. C. Duncan, J. M. Poblet, *J. Am. Chem. Soc.* **2008**, 130, 8223; d) D. Kumar, E. Derat, A. M. Khenkin, R. Neumann, S. Shaik, *J. Am. Chem. Soc.* **2005**, 127, 17712.
- [7] M. T. Pope, *Heteropoly and Isopoly Oxometalates*. Springer, Berlin, **1983**.
- [8] D. L. Kepert, *Prog. Inorg. Chem.* **1962**, 4, 199.
- [9] K. H. Tytko, O. Glemser, *Adv. Inorg. Chem. Radiochem.* **1976**, 19, 239.
- [10] E. Balogh, T. M. Anderson, J. R. Rustad, M. Nyman, W. H. Casey, *Inorg. Chem.* **2007**, 46, 7032.
- [11] M. Filowitz, R. K. C. Ho, W. G. Klemperer, W. Shum, *Inorg. Chem.* **1979**, 18, 93.

- [12] a) M. Iannuzzi, A. Laio, M. Parrinello, *Phys. Rev. Lett.* **2003**, *90*, 238302; b) A. Laio, A. Rodriguez-Fortea, F. L. Gervasio, M. Ceccarelli, M. Parrinello, *J. Phys. Chem. B* **2005**, *109*, 6714.
- [13] A. Rodriguez-Fortea, L. Vilà-Nadal, J. M. Poble, *Inorg. Chem.* **2008**, *47*, 7745.
- [14] Three collective variables (CV) were used: the coordination number of each W atom with respect to the eight O atoms that belong to WO₄ groups and a conditioned CN that counts the number of H atoms bonded to those O atoms bonded to W (see the Supporting Information for more information about the parameters of this and other metadynamics runs).
- [15] a) A. Rodriguez-Fortea, M. Iannuzzi, *J. Phys. Chem. C* **2008**, *112*, 19642; b) J. Blumberger, B. Ensing, M. L. Klein, *Angew. Chem.* **2006**, *118*, 2959; *Angew. Chem. Int. Ed.* **2006**, *45*, 2893.
- [16] J. Schemberg, K. Schneider, U. Demmer, E. Warkentin, A. Müller, U. Ermler, *Angew. Chem.* **2007**, *119*, 2460; *Angew. Chem. Int. Ed.* **2007**, *46*, 2408.
- [17] ADF 2004.01, Department of Theoretical Chemistry, Vrije Universiteit, Amsterdam.
- [18] a) A. D. Becke, *Phys. Rev. A* **1988**, *38*, 3098; b) J. P. Perdew, *Phys. Rev. B* **1986**, *33*, 8822; c) C. Lee, W. Yang, R. Parr, *Phys. Rev. B* **1988**, *37*, 785.
- [19] A. Klamt, G. Schuurmann, *J. Chem. Soc. Perkin Trans. 2* **1993**, 799.
- [20] CPMD, IBM Corp 1990–2006, MPI für Festkörperforschung Stuttgart 1997–2001.
- [21] N. Troullier, J. L. Martins, *Phys. Rev. B* **1991**, *43*, 1993.
-